Applied Thermal Engineering 125 (2017) 1345–1353

Contents lists available at ScienceDirect

Applied Thermal Engineering

journal homepage: www.elsevier.com/locate/apthermeng

Research Paper

Linear method for the design of shell and tube heat exchangers including fouling modeling

Julia C. Lemos [a], André L.H. Costa [a,*], Miguel J. Bagajewicz [b]

[a] Rio de Janeiro State University (UERJ), Rua São Francisco Xavier, 524, Maracanã, CEP, 20550-900, Rio de Janeiro, RJ, Brazil
[b] School of Chemical, Biological and Materials Engineering, University of Oklahoma, Norman, OK 73019, USA

HIGHLIGHTS

- A fouling model is inserted into the design optimization of heat exchangers.
- The mathematical problem consists in a mixed-integer linear programming (MILP).
- The results indicate a better performance when compared to conventional approaches.

ARTICLE INFO

Article history:
Received 7 February 2017
Revised 7 June 2017
Accepted 9 July 2017
Available online 11 July 2017

ABSTRACT

Typical heat exchanger design procedures are based on the use of fixed values of fouling factors, mostly based on estimates coming from practice. However, fouling depends on thermofluidynamic conditions (e.g. flow velocity) which values are consequence of the selection of design variables (e.g. baffle spacing). Therefore, the inclusion of fouling models into an optimal design procedure may yield better solutions. In this article, we extend a recent globally optimal linear formulation for the design of shell and tube heat exchangers (Gonçalves et al., 2017). Our extension leads to a linear model and consists on adding velocity dependent fouling factors. A comparison with design examples based on fixed fouling factors indicates that the linear problem can identify better design solutions, without involving any external convergence loop.

1. Introduction

Heat exchanger design is a very important problem in the chemical process industry. The classical way of solving it is by trial and verification procedures, as in Kern [1], where one first guesses the overall heat transfer coefficient, then chooses the heat exchanger geometry according to the required area and then calculates the overall heat transfer coefficient associated to this tentative heat exchanger. If the solution candidate does not fulfill the service specifications, it is then modified aiming to correct the problems observed. The procedure is repeated until a feasible solution is found. These trial procedures are still presented in more recent books [2,3].

Departing from trial and error procedures, there are many works that explore the heat exchanger design as an optimization problem [4]. The solution of this optimization problem is addressed in the literature using three different approaches: heuristic procedures using thermofluidynamic relations, meta-heuristic methods and mathematical programming.

The heuristic procedures use thermal and hydraulic equations to guide a search path along the space of heat exchanger alternatives. The graphical representation of the search space is a resource commonly employed in this approach [5,6].

The meta-heuristic methods consist in algorithms containing randomized steps that mimic a natural phenomenon, such as, simulated annealing [7], genetic algorithms [8], and particle swarm optimization [9].

The mathematical programming approach has evolved from the analysis of the problem using only continuous variables, yielding nonlinear programming (NLP) models [10,11] to more realistic formulations considering the presence of integer and continuous variables, therefore involving mixed-integer nonlinear programming (MINLP) models [12–14]. However, those models are nonconvex and therefore do not guarantee to find the global optimum when local solvers are used. Recently, a third generation of mathematical programming models for heat exchanger design was proposed by Gonçalves et al. [15,16] represented by mixed-integer linear programming (MILP) and integer linear programming (ILP) rigorous formulations; because it is linear, it guarantees global optimality.

* Corresponding author.
E-mail address: andrehc@uerj.br (A.L.H. Costa).

http://dx.doi.org/10.1016/j.applthermaleng.2017.07.066
1359-4311/

Nomenclature

A	area (m^2)
$\widehat{Aexc}$	excess area (%)
$Areq$	required area (m^2)
Ar	area between adjacent baffles (m^2)
dte	outer tube diameter (m)
dti	inner tube diameter (m)
Deq	equivalent diameter (m)
Ds	shell diameter (m)
fs	Darcy friction factor for shell-side
ft	Darcy friction factor for tube-side
F	LMTD correction factor
FAR	free area ratio
$\hat{g}$	gravity acceleration (m/s^2)
hs	convective heat transfer coefficient for shell-side (W/m^2 K)
ht	convective heat transfer coefficient for tube-side (W/m^2 K)
$\widehat{kRfs}$	shell-side fouling model parameter
$\widehat{kRft}$	tube-side fouling model parameter
$\widehat{ks}$	thermal conductivity of the fluid on shell-side (W/m K)
$\widehat{kt}$	thermal conductivity of the fluid on tube-side (W/m K)
$ktube$	thermal conductivity of the tube wall (W/m K)
lay	layout of the heat exchanger
lbc	baffle spacing (m)
ltp	tube pitch (m)
L	tube length (m)
$\widehat{ms}$	mass flow rate on shell-side (kg/s)
$\widehat{mt}$	mass flow rate on tube-side (kg/s)
Nb	number of baffles
Npt	number of tube passes
Ntp	number of tubes per pass
Ntt	total number of tubes
Nus	Nusselt number for shell-side
Nut	Nusselt number for tube-side
$\widehat{PDs}_{srow}$	standard shell diameter (m)
$\widehat{Pdte}_{srow}$	standard outer tube diameter (m)
$\widehat{Pdti}_{srow}$	standard inner tube diameter (m)
$\widehat{PL}_{srow}$	standard tube length (m)
$\widehat{Play}_{srow}$	tube layout
$\widehat{PNb}_{srow}$	number of baffles
$\widehat{PNpt}_{srow}$	number of tube passes
$\widehat{PNtt}_{srow}$	total number of tubes
$\widehat{Prp}_{srow}$	standard tube pitch ratio
$\widehat{Prs}$	Prandtl for shell-side
$\widehat{Prt}$	Prandtl for tube-side
$\hat{Q}$	heat load (W)
rp	pitch ratio
Res	Reynolds number for shell-side
Ret	Reynolds number for tube-side
Rfs	fouling factor on shell-side (m^2 K/W)
Rft	fouling factor on tube-side (m^2 K/W)
$\widehat{Tci}$	cold stream inlet temperature (°C)
$\widehat{Tco}$	cold stream outlet temperature (°C)
$\widehat{Thi}$	hot stream inlet temperature (°C)
$\widehat{Tho}$	hot stream outlet temperature (°C)
U	overall heat transfer coefficient (W/m^2 K)
vs	shell-side flow velocity (m/s)
$\widehat{vsmax}$	maximum shell-side flow velocity (m/s)
$\widehat{vsmin}$	minimum shell-side flow velocity (m/s)
vt	tube-side flow velocity (m/s)
$\widehat{vtmax}$	maximum tube-side flow velocity (m/s)
$\widehat{vtmin}$	minimum tube-side low velocity (m/s)
yd_{sd}	binary variable representing the tube diameter
yDs_{sDs}	binary variable representing the shell diameter
yL_{sL}	binary variable representing the tube length
$ylay_{slay}$	binary variable representing the tube layout
yNb_{sNb}	binary variable representing the number of baffles
$yNpt_{sNpt}$	binary variable representing the number of tube passes
yrp_{srp}	binary variable representing the tube pitch ratio
$yrow_{srow}$	binary variable that represents simultaneously all discrete variables

Greek letters

$\widehat{\alpha Rfs}$	shell-side fouling model parameter
$\widehat{\alpha Rft}$	tube-side fouling model parameter
$\widehat{\Delta Ps}$	pressure drop on shell-side (Pa)
$\widehat{\Delta Psdisp}$	available pressure drop on shell-side (Pa)
ΔPt	pressure drop on tube-side (Pa)
$\widehat{\Delta Ptdisp}$	available pressure drop on tube-side (Pa)
$\widehat{\Delta Tlm}$	logarithmic mean temperature difference (°C)
$\widehat{\mu s}$	viscosity of the fluid on shell-side (Pa s)
$\widehat{\mu t}$	viscosity of the fluid on tube-side (Pa s)
$\widehat{\rho s}$	density of the fluid on the shell-side (kg/m^3)
$\widehat{\rho t}$	density of the fluid on the tube-side (kg/m^3)

Despite the intense research about fouling, heat exchangers are still designed using fixed fouling factors. Therefore, independently of the nature of the search algorithm, the majority of the aforementioned procedures employ constant fouling factors to describe the impact of the accumulation of the deposits on the thermal performance. In addition, fouling factors are associated to a considerable level of uncertainty, which in some cases may lead to poorly designed heat exchangers that will not fulfill their objective correctly. Shilling [17] presented the problems associated to an excessive design margin due to the inadequate selection of fouling factors: unnecessary capital costs, designs with lower velocities susceptible to fouling, and excessive heating or cooling of the process stream.

A limited number of papers has considered the interrelation of fouling models and heat exchanger design. Butterworth [18] analyzed the impact of fouling on the design using a graph relating the number of tubes and tube length, where it is possible to identify how the region containing the feasible design options is modified according to the fouling status. Particularly, it is explored the Ebert-Panchal model [19,20], suitable for crude oil fouling.

Polley et al. [21] explored the analysis of the relation between fouling and design using the same graph representation (Poddar plot) together with the Ebert-Panchal model. In this model, fouling depends on the temperature and flow velocity, as it is illustrated in Fig. 1, where it can be observed a no fouling region (threshold model). Despite the existence of this region, the threshold velocity may be too high when considering hydraulic, vibrational and erosional limitations, thus imposing a design with fouling presence.

Polley et al. [22] discussed the design of heat exchangers to achieve an operating period in a refinery preheat train. They propose a procedure to design the heat exchanger for the clean condition and afterwards increase its size to be able to achieve the needed heat load during the entire operating period, while considering a fouling model to predict the fouling factor. They discuss that even with the procedure there is a risk of needing unscheduled cleanings, where this risk decreases with the increase of the exchanger size. They also discuss the use of tube inserts and uncertainties.

Nakao et al. [23] presented an iterative scheme based on the update of fouling factors in a heat exchanger design algorithm

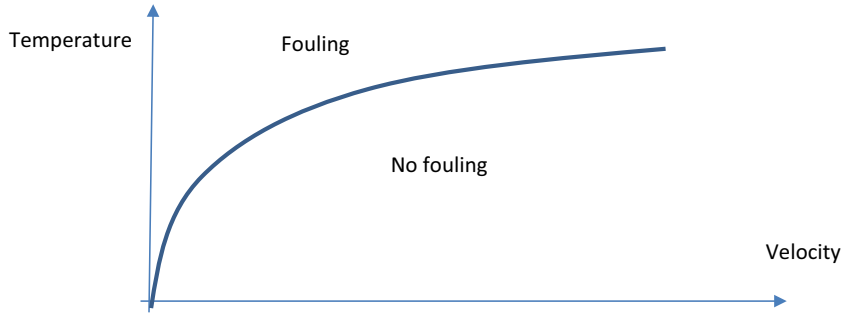

Fig. 1. Fouling threshold model.

employing a fouling rate model. At each iteration, the heat exchanger is simulated during the operational period to determine the fouling factors at the end of the campaign.

As it was illustrated above, the analysis of the literature indicates that the efforts to insert fouling models in heat exchanger design are dominated by heuristic approaches. As far as we know, a more rigorous mathematical treatment of the heat exchanger equations and fouling modelling for the solution of the optimal design problem was not proposed yet. In order to fill this gap, in this article we extend the linear formulation presented by Gonçalves et al. [15,16] to design heat exchangers, including a fouling behavior equation, instead to use fixed fouling factors. This insertion preserves the linearity of the model, therefore the results are still globally optimal. We show that the results of using fixed values of fouling factors, like those suggested by TEMA or others, can lead to significant area discrepancies when compared to results obtained using a model that actually calculates these fouling factors during the design procedure.

The rest of the article is organized as follows: for completion, we first present in Section 2 the original non-linear heat exchanger model we are using followed by a brief discussion on fouling models in Section 3. The development of the linear formulation including the model with fouling factors as a function of velocity is described in Section 4. In Section 5, we show results for different cases, including an alternative iterative procedure and compare it with the proposed solution. Finally, Section 6 contains the conclusions.

2. Heat exchanger model

We consider heat exchangers with a single E-shell type processing fluids that do not go into phase change. The number of tube passes is one or an even number (2, 4, 6, ...). We assume that the flow regime is turbulent, which is the most common in industry. We used the Kern model equations [1] and the Dittus-Boelter as well as the Darcy-Weisbach equations for the calculations of heat transfer coefficients and pressure drop [24,25]. Fluid allocation is considered to be a parameter, which is determined prior the optimization by the designer. Finally, the problem parameters, which are fixed prior the optimization, are represented using the symbol "^" on top.

We now present all the nonlinear equations of the heat exchanger model that will serve as base to the development of the linear model that will be shown later.

2.1. Shell-side thermal and hydraulic equations

The Nusselt number for shell-side is given by [1]:

$$Nus = 0.36 Res^{0.55} \widehat{Prs}^{1/3} \tag{1}$$

where $\widehat{Prs}$ is the dimensionless group Prandtl and Res is the Reynolds number. The Nusselt number and the Reynolds number are defined as:

$$Nus = \frac{hs\ Deq}{\widehat{ks}} \tag{2}$$

$$Res = \frac{Deq\ vs\ \widehat{\rho s}}{\widehat{\mu s}} \tag{3}$$

where $\widehat{ks}$, $\widehat{\rho s}$ and $\widehat{\mu s}$ are the thermal conductivity, the density and the viscosity of the fluid, respectively. Regarding the variables, hs is the convective heat transfer coefficient, Deq is the equivalent diameter and vs is the flow velocity.

The equivalent diameter is a function of the outer tube diameter (dte) and the tube pitch (ltp), and also depends on the layout of the heat exchanger.

$$Deq = \frac{4\ ltp^2}{\pi\ dte} - dte \quad \text{(Square pattern)} \tag{4}$$

$$Deq = \frac{3.46\ ltp^2}{\pi\ dte} - dte \quad \text{(Triangular pattern)} \tag{5}$$

The flow velocity is given by:

$$vs = \frac{\widehat{ms}}{\widehat{\rho s}\ Ar} \tag{6}$$

where $\widehat{ms}$ is the shell-side mass flow rate and Ar is the flow area between adjacent baffles, which can be described by:

$$Ar = Ds\ FAR\ lbc \tag{7}$$

where Ds is the shell diameter, lbc is the baffle spacing and FAR is the free area ratio, that is given by:

$$FAR = \frac{(ltp - dte)}{ltp} = 1 - \frac{dte}{ltp} = 1 - \frac{1}{rp} \tag{8}$$

The pressure drop in the shell-side flow ΔPs, not considering nozzle pressure drop, can be described by the next equation [1], where fs is the shell-side friction factor and Nb is the number of baffles. The equations that describe the friction factor and the relation between the number of baffles and the tube length (L) are also shown below:

$$\frac{\Delta Ps}{\widehat{\rho s}\ \hat{g}} = fs \frac{Ds(Nb+1)}{Deq}\left(\frac{vs^2}{2\hat{g}}\right) \tag{9}$$

$$fs = 1.728 Res^{-0.188} \tag{10}$$

$$Nb = \frac{L}{lbc} - 1 \tag{11}$$

2.2. Tube-side thermal and hydraulic equations

The tube-side Nusselt number (Nut) is given by the Dittus-Boelter correlation [25]:

$$Nut = 0.023 Ret^{0.8} \widehat{Prt}^{n} \tag{12}$$

$$Nut = \frac{ht\ dti}{\widehat{kt}} \tag{13}$$

where the parameter n is equal to 0.3 for cooling services and 0.4 for heating services. The Reynolds number is given by:

$$Ret = \frac{dti\ vt\ \widehat{\rho t}}{\widehat{\mu t}} \tag{14}$$

where the parameters $\widehat{\mu t}$ and $\widehat{\rho t}$ are the viscosity and the density of the tube-side stream, respectively. The variable dti is the inner tube diameter and vt is the tube-side flow velocity:

$$vt = \frac{4\widehat{mt}}{Ntp\ \pi\ \widehat{\rho t}\ dti^2} \tag{15}$$

where $\widehat{mt}$ is the mass flow rate and Ntp is the number of tubes per pass.

The pressure drop in the tube-side flow (ΔPt), considering constant physical properties, is given by [24]:

$$\frac{\Delta P\ t}{\widehat{\rho t}\ \hat{g}} = \frac{ft\ Npt\ L\ vt^2}{2\ \hat{g}\ dti} + \frac{K\ Npt\ vt^2}{2\ \hat{g}} \tag{16}$$

where ft is the tube-side friction factor. This equation considers the head loss in the tube bundle, first term in the right hand side, and the head loss in the front and rear headers, in the second term. The parameter K is determined by the number of tube passes and is equal to 0.9 for one tube pass and 1.6 for two or more.

The Darcy friction factor for turbulent flow is [24]:

$$ft = 0.014 + \frac{1.056}{Ret^{0.42}} \tag{17}$$

2.3. Overall heat transfer coefficient

The expression of the overall heat transfer coefficient (U) is:

$$U = \frac{1}{\frac{dte}{dtiht} + \frac{\widehat{Rft}\,dte}{dti} + \frac{dte \ln\left(\frac{dte}{dti}\right)}{2\widehat{ktube}} + \widehat{Rfs} + \frac{1}{hs}} \tag{18}$$

where $\widehat{Rft}$ and $\widehat{Rfs}$ are the fouling factors of the tube-side and shell-side streams, respectively, and $\widehat{ktube}$ is the thermal conductivity of the tube wall.

2.4. Heat transfer rate equation

The LMTD method is based on the logarithmic mean temperature difference ($\widehat{\Delta Tlm}$) described by:

$$\widehat{\Delta Tlm} = \frac{(\widehat{Thi} - \widehat{Tco}) - (\widehat{Tho} - \widehat{Tci})}{\ln\left(\frac{(\widehat{Thi} - \widehat{Tco})}{(\widehat{Tho} - \widehat{Tci})}\right)} \tag{19}$$

The heat transfer rate equation is given by:

$$\hat{Q} = UAreq\widehat{\Delta Tlm}\ F \tag{20}$$

where $\hat{Q}$ is the heat load, $Areq$ is the required area and F is the LMTD correction factor.

This correction factor is equal to 1 if the heat exchanger has only one tube pass in countercurrent flow, otherwise it is described by the following equation for an even number of tube passes:

$$F = \frac{(\hat{R}^2+1)^{0.5} \ln\left(\frac{(1-\hat{P})}{(1-\hat{R}\hat{P})}\right)}{(\hat{R}-1)\ln\left(\frac{2-\hat{P}(\hat{R}+1-(\hat{R}^2+1)^{0.5})}{2-\hat{P}(\hat{R}+1+(\hat{R}^2+1)^{0.5})}\right)} \tag{21}$$

where

$$\hat{R} = \frac{\widehat{Thi} - \widehat{Tho}}{\widehat{Tco} - \widehat{Tci}} \tag{22}$$

$$\hat{P} = \frac{\widehat{Tco} - \widehat{Tci}}{\widehat{Thi} - \widehat{Tci}} \tag{23}$$

The heat transfer area (A) is given by:

$$A = Ntt\ \pi\ dte\ L \tag{24}$$

where Ntt is the total number of tubes.

The heat exchanger area must be higher than the required area aiming to guarantee a design margin according to a certain "excess area" ($\widehat{Aexc}$):

$$A \geqslant \left(1 + \frac{\widehat{Aexc}}{100}\right) Areq \tag{25}$$

2.5. Bounds on pressure drops, flow velocities and Reynolds numbers

The pressure drop and flow velocity have lower and upper bounds, which should be taken into the model:

$$\Delta Ps \leqslant \widehat{\Delta Psdisp} \tag{26}$$

$$\Delta Pt \leqslant \widehat{\Delta Ptdisp} \tag{27}$$

$$\widehat{vsmin} \leqslant vs \leqslant \widehat{vsmax} \tag{28}$$

$$\widehat{vtmin} \leqslant vt \leqslant \widehat{vtmax} \tag{29}$$

The correlations for the convective heat transfer coefficient are associated to the following validity ranges:

$$Res \geqslant 2 \cdot 10^3 \tag{30}$$

$$Ret \geqslant 10^4 \tag{31}$$

2.6. Geometric constraints

The baffle spacing must be limited between 20% and 100% of the shell diameter [26]:

$$lbc \geqslant 0.2Ds \tag{32}$$

$$lbc \leqslant 1.0Ds \tag{33}$$

The ratio between the tube length and shell diameter must be between 3 and 15 [27]:

$$L \geqslant 3Ds \tag{34}$$

$$L \leqslant 15Ds \tag{35}$$

2.7. Objective function

Two alternative objective functions can be considered in the analysis of the optimization of the heat exchanger design: the min-

imization of the heat exchanger area for a given set of maximum pressure drops or the minimization of the total annualized costs encompassing capital and operating costs (in this case, the pressure drop bounds are excluded). These objective functions are represented, respectively, by:

$$\min A \tag{36}$$

$$\min \hat{a}_{cost} A^{0.59} + \hat{p}_{cost}\left(\Delta Pt \frac{\widehat{mt}}{\widehat{\rho t}} + \Delta Ps \frac{\widehat{ms}}{\widehat{\rho s}}\right) \tag{37}$$

where $\hat{a}_{cost}$ and $\hat{p}_{cost}$ are cost parameters related to capital and operating costs, respectively [12].

3. Fouling models

Fouling has a direct impact on heat exchanger performance; therefore, its importance should not be neglected in the heat exchanger design. In order to include its behavior on an exchanger model, one should know which variables may influence it in the particular service chosen and to propose a quantitative relation between fouling resistance and these variables.

Many works focus on fouling behavior, trying to achieve a fouling model that describes how the fouling resistance varies with time, fluid properties, temperature, and fluidynamic conditions. These models vary from simple linear models to complex ones like the Ebert and Panchal model [28] and its variants [29–31] that were reviewed by Wilson et al. [19,20].

The proposed approach does not involve the utilization of fouling rate models. The formulation of the optimization problem explores the relation between the asymptotic fouling resistance and flow velocity. An example of such model, it is presented in Nesta and Bennett [32]:

$$Rft = \widehat{kRft}(vt)^{-\widehat{\alpha Rft}} \tag{38}$$

where $\widehat{kRft}$ and $\widehat{\alpha Rft}$ are the parameters of the model.

Nesta and Bennett [32] have used this model for cooling water fouling in the tube-side. In this work, we make the assumption that such power-law behavior could be used for both sides of the heat exchanger involving also other streams [33].

4. Linear model

The model that will be developed is an extension of the one proposed by Gonçalves et al. [15,16], where it is proposed here the inclusion of a fouling model without losing the linear nature of the original formulation.

The discrete geometric variables and the representation of the list of possible values for each one of them are inner and outer tube diameters ($\widehat{pdti}$ and $\widehat{pdte}$), shell diameter ($\widehat{pDs}$), number of tube passes ($\widehat{pNpt}$), pitch ratio ($\widehat{prp}$), layout ($\widehat{play}$), tube length ($\widehat{pL}$) and number of baffles ($\widehat{pNb}$). The constraints that represent each one of these geometric variables are displayed in the following equations involving binary variables:

$$dte = \sum_{sd=1}^{sdmax} \widehat{pdte}_{sd} yd_{sd} \tag{39}$$

$$dti = \sum_{sd=1}^{sdmax} \widehat{pdti}_{sd} yd_{sd} \tag{40}$$

$$Ds = \sum_{sDs=1}^{sDsmax} \widehat{pDs}_{sDs} yDs_{sDs} \tag{41}$$

$$lay = \sum_{slay=1}^{slaymax} \widehat{play}_{slay} ylay_{slay} \tag{42}$$

$$Npt = \sum_{sNpt=1}^{sNptmax} \widehat{pNpt}_{sNpt} yNpt_{sNpt} \tag{43}$$

$$rp = \sum_{srp=1}^{srpmax} \widehat{prp}_{srp} yrp_{srp} \tag{44}$$

$$L = \sum_{sL=1}^{sLmax} \widehat{pL}_{sL} yL_{sL} \tag{45}$$

$$Nb = \sum_{sNb=1}^{sNbmax} \widehat{pNb}_{sNb} yNb_{sNb} \tag{46}$$

The binary variables, represented by y in Eqs. (39)–(46), must obey Eqs. (47)–(53) to map only one option for the heat exchanger solution:

$$\sum_{sd=1}^{sdmax} yd_{sd} = 1 \tag{47}$$

$$\sum_{sDs=1}^{sDsmax} yDs_{sDs} = 1 \tag{48}$$

$$\sum_{slay=1}^{slaymax} ylay_{slay} = 1 \tag{49}$$

$$\sum_{sNpt=1}^{sNptmax} yNpt_{sNpt} = 1 \tag{50}$$

$$\sum_{srp=1}^{srpmax} yrp_{srp} = 1 \tag{51}$$

$$\sum_{sL=1}^{sLmax} yL_{sL} = 1 \tag{52}$$

$$\sum_{sNb=1}^{sNbmax} yNb_{sNb} = 1 \tag{53}$$

As shown by Gonçalves et al. [16], to solve the problem faster, one can consider only one set of binary variables, where the discrete variables are all represented by this unique set with a multi-index *srow* = (*sd, sDs, slay, sNpt, srp, sL, sNb*). This new index, which replaces all the previous indexes related to each one of the geometric variables, represents the rows of a table that contains all the possible combinations of the geometric variables, as illustrated in Fig. 2.

Therefore, the new parameters that represent the commercial values of the design variables will be:

$$\widehat{Pdte}_{srow} = \widehat{pdte}_{sd} \tag{54}$$

$$\widehat{Pdti}_{srow} = \widehat{pdti}_{sd} \tag{55}$$

$$\widehat{PDs}_{srow} = \widehat{pDs}_{sDs} \tag{56}$$

$$\widehat{Play}_{srow} = \widehat{play}_{slay} \tag{57}$$

$$\begin{array}{cccccccc}
\widehat{Pdte}_1 & \widehat{Pdti}_1 & \widehat{PDs}_1 & \cdots & \cdots & \cdots & \widehat{PL}_1 & \widehat{PNb}_1 \\
\widehat{Pdte}_1 & \widehat{Pdti}_1 & \widehat{PDs}_1 & \cdots & \cdots & \cdots & \widehat{PL}_1 & \widehat{PNb}_2 \\
\widehat{Pdte}_1 & \widehat{Pdti}_1 & \widehat{PDs}_1 & \cdots & \cdots & \cdots & \widehat{PL}_1 & \widehat{PNb}_3 \\
\vdots & \vdots & \vdots & \ddots & & & & \\
\vdots & \vdots & \vdots & & \ddots & & \vdots & \vdots \\
\vdots & \vdots & \vdots & & & \ddots & & \\
\widehat{Pdte}_{n-1} & \widehat{Pdti}_{n-1} & \widehat{PDs}_n & \cdots & \cdots & \cdots & \widehat{PL}_n & \widehat{PNb}_n \\
\widehat{Pdte}_n & \widehat{Pdti}_n & \widehat{PDs}_n & \cdots & \cdots & \cdots & \widehat{PL}_n & \widehat{PNb}_n
\end{array}$$

Fig. 2. Representation of the multi-indexed search space.

$$\widehat{PNpt}_{srow} = \widehat{pNpt}_{sNpt} \tag{58}$$

$$\widehat{Prp}_{srsrow} = \widehat{prp}_{srp} \tag{59}$$

$$\widehat{PL}_{srow} = \widehat{pL}_{sL} \tag{60}$$

$$\widehat{PNb}_{srow} = \widehat{pNb}_{sNb} \tag{61}$$

Instead of having Eqs. (39)–(53), the geometric variables will be represented by the following equations:

$$dte = \sum_{srow} \widehat{Pdte}_{srow} yrow_{srow} \tag{62}$$

$$dti = \sum_{srow} \widehat{Pdti}_{srow} yrow_{srow} \tag{63}$$

$$Ds = \sum_{srow} \widehat{PDs}_{srow} yrow_{srow} \tag{64}$$

$$lay = \sum_{srow} \widehat{Play}_{srow} yrow_{srow} \tag{65}$$

$$Npt = \sum_{srow} \widehat{PNpt}_{srow} yrow_{srow} \tag{66}$$

$$rp = \sum_{srow} \widehat{Prp}_{srow} yrow_{srow} \tag{67}$$

$$L = \sum_{srow} \widehat{PL}_{srow} yrow_{srow} \tag{68}$$

$$Nb = \sum_{srow} \widehat{PNb}_{srow} yrow_{srow} \tag{69}$$

$$\sum_{srow} yrow_{srow} = 1 \tag{70}$$

The idea of Gonçalves et al. [16] is to substitute the linear Eqs. (62)–(70) into the nonlinear heat exchanger model displayed in Eqs. (1)–(37), making the necessary arrangements to have a linear model.

Here, we only show the derivation of the new equations, related to the fouling model, that we proposed to be inserted into the heat exchanger design problem. The remaining model equations, that were not modified, can be found in Gonçalves et al. [16]. The complete set of equations can be also accessed in Supplementary Material.

The linear form of the velocity equations are:

$$vs = \frac{\widehat{ms}}{\widehat{\rho s}} \sum_{srow} \frac{(\widehat{PNb}_{srow} + 1)}{\widehat{PDs}_{srow} \widehat{PFAR}_{srow} \widehat{PL}_{srow}} yrow_{srow} \tag{71}$$

$$vt = \frac{4\widehat{mt}}{\pi \widehat{\rho t}} \sum_{srow} \frac{\widehat{PNpt}_{srow}}{\widehat{PNtt}_{srow} \widehat{Pdti}^2_{srow}} yrow_{srow} \tag{72}$$

The equivalent linear equation, based on fixed values of fouling factors, for the design equation corresponding to Eq. (20) is:

$$\begin{aligned}
&\hat{Q}\left(\sum_{srow} \frac{\widehat{Pdte}_{srow}}{\widehat{Pht}_{srow} \widehat{Pdti}_{srow}} yrow_{srow} + \widehat{Rft} \sum_{srow} \frac{\widehat{Pdte}_{srow}}{\widehat{Pdti}_{srow}} yrow_{srow}\right. \\
&\quad \left. + \sum_{srow} \frac{\widehat{Pdte}_{srow}}{2\widehat{ktube}} In\left(\frac{\widehat{Pdte}_{srow}}{\widehat{Pdti}_{srow}}\right) yrow_{srow} + \widehat{Rfs} + \sum_{srow} \frac{1}{\widehat{Phs}_{srow}} yrow_{srow}\right) \\
&\leqslant \left(\frac{100}{100 + \widehat{Aexc}}\right)\left(\pi \sum_{srow} \widehat{PNtt}_{srow} \widehat{Pdte}_{srow} \widehat{PL}_{srow} yrow_{srow}\right) \cdot \widehat{\Delta Tlm} \hat{F}_{srow}
\end{aligned} \tag{73}$$

The fouling factor expressions, after the velocity equations have been substituted and further linearized become:

$$Rfs = \widehat{kRfs} \left(\frac{\widehat{ms}}{\widehat{\rho s}}\right)^{-\widehat{\alpha Rfs}} \sum_{srow} \left(\frac{(\widehat{PNb}_{srow} + 1)}{\widehat{PDs}_{srow} \widehat{PFAR}_{srow} \widehat{PL}_{srow}}\right)^{-\widehat{\alpha Rfs}} yrow_{srow} \tag{74}$$

$$Rft = \widehat{kRft} \left(\frac{4\widehat{mt}}{\pi \widehat{\rho t}}\right)^{-\widehat{\alpha Rft}} \sum_{srow} \left(\frac{\widehat{PNpt}_{srow}}{\widehat{PNtt}_{srow} \widehat{Pdti}^2_{srow}}\right)^{-\widehat{\alpha Rft}} yrow_{srow} \tag{75}$$

Once Eqs. (74) and (75) are inserted in Eq. (73), we get the following heat transfer rate equation:

$$\begin{aligned}
&\hat{Q}\left(\sum_{srow} \frac{\widehat{Pdte}_{srow}}{\widehat{Pht}_{srow} \widehat{Pdti}_{srow}} yrow_{srow} + \widehat{kRft} \left(\frac{4\widehat{mt}}{\pi \widehat{\rho t}}\right)^{-\widehat{\alpha Rft}}\right. \\
&\quad \times \sum_{srow} \left(\frac{\widehat{PNpt}_{srow}}{\widehat{PNtt}_{srow} \widehat{Pdti}^2_{srow}}\right)^{-\widehat{\alpha Rft}} \frac{\widehat{Pdte}_{srow}}{\widehat{Pdti}_{srow}} yrow_{srow} \\
&\quad + \sum_{srow} \frac{\widehat{Pdte}_{srow}}{2\widehat{ktube}} In\left(\frac{\widehat{Pdte}_{srow}}{\widehat{Pdti}_{srow}}\right) yrow_{srow} \\
&\quad + \widehat{KRfs} \left(\frac{\widehat{ms}}{\widehat{\rho s}}\right)^{-\widehat{\alpha Rfs}} \sum_{srow} \left(\frac{(\widehat{PNb}_{srow} + 1)}{\widehat{PDs}_{srow} \widehat{PFAR}_{srow} \widehat{PL}_{srow}}\right)^{-\widehat{\alpha Rfs}} yrow_{srow} \\
&\quad \left. + \sum_{srow} \frac{1}{\widehat{Phs}_{srow}} yrow_{srow}\right) \\
&\leqslant \left(\frac{100}{100 + \widehat{Aexc}}\right)\left(\pi \sum_{srow} \widehat{PNtt}_{srow} \widehat{Pdte}_{srow} \widehat{PL}_{srow} yrow_{srow}\right) \cdot \widehat{\Delta Tlm} \hat{F}_{srow}
\end{aligned} \tag{76}$$

5. Results

In this section, we present the results for solving the linear problem extended to include the fouling behavior, as it is proposed in the current paper. Aiming to illustrate the advantage of the proposed approach, we also solved the design problem using the linear formulation, but using fixed fouling resistances, as it is the common practice. The definition of the fixed fouling resistance values was based on the fouling model, adopting the lowest (pessimist) and highest (optimistic) values of flow velocities. Additionally, we also considered an iterative procedure that could be applied to the linear model with fixed fouling resistances (an adaptation of the procedure proposed by Nakao et al. [23]). These analyses were conducted considering the minimization of the heat

transfer area. In a last investigated case, we present the results of the optimization procedure based on the minimization of the total annualize cost.

The example investigated considers that the fluid flowing on both sides of the heat exchanger is water, and the cold fluid is in the tube-side. Table 1 presents the physical properties of the streams, Table 2 displays the characteristics of the thermal service, and Table 3 presents the alternatives of discrete values of the geometric variables.

The values used for the fouling model constants were the ones reported by Nesta and Bennett [32]. These values were considered to be the same for both sides of the heat exchanger, with $\widehat{kRft}$ and $\widehat{kRfs}$ assuming a value of 0.00062, and $\widehat{\alpha Rft}$ and $\widehat{\alpha Rfs}$ equal to 1.65. We consider that the area must be 11% larger than the required area (design margin). All the problems were solved using the software GAMS with the solver CPLEX.

5.1. Case 1: Optimization with fixed fouling resistances calculated using the lowest flow velocities

The first case considers the fouling resistances constant and their values are calculated prior the optimization using Eq. (38) in a worst-case scenario (fouling resistances based on the velocity lower bounds). As a result, the fouling resistance on the tube-side is equal to $6.20 \cdot 10^{-4}$ m^2 K/W and on the corresponding value in the shell-side is $1.9458 \cdot 10^{-3}$ m^2 K/W. The optimization results are presented on Table 4.

This solution was obtained using a given pair of fouling resistances, but to analyze the results and verify if the area found is larger than the area really needed, we calculate the fouling resistance with Eq. (38) applied to both tube and shell sides using the actual velocity, according to the design found and recalculate the heat transfer coefficients. The results are in Table 5.

We can observe that the *Rf* values corresponding to the actual flow velocities would be smaller than those assumed at the beginning and, therefore, in a trial and verify context, this exchanger is acceptable. The remaining question is if the area is close to a minimum possible value.

Table 1
Water physical properties.

Density (kg/m^3)	Viscosity (Pa s)	Conductivity (W/m K)	Heat capacity (J/kg K)
1000	0.000695	0.628	4178

Table 2
Thermal service.

	Cold stream	Hot stream
Mass flow rate (kg/s)	200	100
Inlet temperature (°C)	32	70
Outlet temperature (°C)	40	54
Maximum pressure drop (kPa)	100	100
Flow velocity bounds (m/s)	1.0–3.0	0.5–2.0

Table 3
Alternatives of discrete values of the geometric variables.

Variable	Values
Tube outer diameter, $\widehat{pdte}_{sd}$ (m)	0.01905, 0.02540, 0.03175, 0.03810, 0.05080
Tube inner diameter, $\widehat{pdti}_{sd}$ (m)	0.01575, 0.02210, 0.02845, 0.03480, 0.04750
Tube length, $\widehat{pL}_{sL}$ (m)	1.2195, 1.8293, 2.4390, 3.0488, 3.6585, 4.8768, 6.0976
Number of baffles, $\widehat{pNb}_{sNb}$	1,2,...,20
Number of tube passes, $\widehat{pNpt}_{sNpt}$	1, 2, 4, 6
Tube pitch ratio, $\widehat{prp}_{srp}$	1.25, 1.33, 1.50
Shell diameter, $\widehat{pDs}_{sDs}$ (m)	0.7874, 0.8382, 0.889, 0.9398, 0.9906, 1.0668, 1.143, 1.2192, 1.3716, 1.524
Tube layout, $\widehat{play}_{slay}$	1 = square, 2 = triangular

Table 4
Results for case 1.

Variable	Value	Variable	Value
dte (m)	0.01905	*Deq* (m)	0.01375
dti (m)	0.01575	*Res*	10,647
L (m)	4.8768	*Nus*	98.38
Nb	7	*hs* (W/m^2 K)	4494.0
Npt	4	*vt* (m/s)	1.23
rp	1.25	*Ret*	27857.9
Ds (m)	1.524	*Nut*	152.6
lay	2	*ht* (W/m^2 K)	6086.4
ltp (m)	0.02381	*U* (W/m^2 K)	317.14
Ntt	3342	*A* (m^2)	974.9
Ntp	835.5	*fs*	0.3023
ebc (m)	0.6096	*ft*	0.02835
Ar (m^2)	0.1858	ΔPs (Pa)	38822
vs (m/s)	0.5382	ΔPt (Pa)	31,364

5.2. Case 2: Optimization with fixed fouling resistances calculated using the highest flow velocities

The second case considers the best-case scenario, using the velocity upper bounds to calculate the fouling resistances prior the optimization. The fouling resistances are considered constant and equal to the values calculated through Eq. (38): $1.01 \cdot 10^{-4}$ m^2 K/W in the tube-side and $1.97 \cdot 10^{-4}$ m^2 K/W in the shell-side. Table 6 presents the results and Table 7 shows the recalculation using the same procedure as the previous case.

Table 5
Recalculation according to the fouling model.

Variable	Calculated value
Rft (m^2 K/W)	$4.41 \cdot 10^{-4}$
Rfs (m^2 K/W)	$1.723 \cdot 10^{-3}$
New *U* (W/m^2 K)	363.42

Table 6
Results for case 2.

Variable	Value	Variable	Value
dte (m)	0.01905	*Deq* (m)	0.01375
dti (m)	0.01575	*Res*	17168.4
L (m)	3.6585	*Nus*	127.9
Nb	4	*hs* (W/m^2 K)	5844.6
Npt	2	*vt* (m/s)	2.303
rp	1.25	*Ret*	52186.7
Ds (m)	0.7874	*Nut*	252.2
lay	2	*ht* (W/m^2 K)	10056.6
ltp (m)	0.02381	*U* (W/m^2 K)	1544.3
Ntt	892	*A* (m^2)	195.2
Ntp	446	*fs*	0.2763
ebc (m)	0.7317	*ft*	0.02502
Ar (m^2)	0.1152	ΔPs (Pa)	29796
vs (m/s)	0.868	ΔPt (Pa)	39309

Table 7
Recalculation according to the fouling model.

Variable	Calculated value
Rft (m^2 K/W)	$1.5655 \cdot 10^{-4}$
Rfs (m^2 K/W)	$7.8336 \cdot 10^{-4}$
U (W/m^2 K)	775.8

In this case study, the calculated fouling resistances are smaller than those used to design the exchanger and a new trial would be needed, i.e. this heat exchanger design proposal is not feasible.

5.3. Case 3: Optimization with fixed fouling resistances updated using a iterative process

In this case, we performed an iterative procedure that updates the fouling resistance values. This procedure consists of solving a sequence of optimization problems with fixed fouling resistances, where the corresponding fouling values are calculated prior the optimization through Eq. (38) using the velocities obtained in the previous iteration. If the procedure does not converge, the solution selected is the alternative visited with the smallest area such that its fouling resistances calculated at the end of the iteration (function of the velocities) are smaller than the ones adopted at the beginning of the iteration. Therefore, this heat exchanger alternative is feasible, because the fouling resistances during the operational campaign will be lower than those adopted in the design.

This design procedure was applied using 11 different initial estimates of fouling resistances based on equally spaced flow velocities distributed along the interval limited by the lower and upper bounds (i.e. a 10% increment). For a limit of 20 maximum iterations, there was no convergence in any run (the iterative sequences assume a cycling pattern). The analysis of the results indicate the identification of two solutions with 493.6 m^2 and 506.6 m^2. The details of the best solution are shown in Table 8.

5.4. Case 4: Optimization extended to include the fouling model

Here, the developed linear model was used to find the global optimum for the presented problem. The results are depicted in Table 9.

5.5. Comparison among the different solution approaches

The proposed optimization scheme is composed of 168,000 binary variables and 477,253 constraints. Table 10 presents a comparison of its performance with the other approaches discussed above.

Table 9
Results for case 4.

Variable	Value	Variable	Value
dte (m)	0.0254	*Deq* (m)	0.02516
dti (m)	0.0221	*Res*	33483.6
L (m)	4.8768	*Nus*	184.8
Nb	10	*hs* (W/m^2 K)	4612.3
Npt	4	*vt* (m/s)	2.00
rp	1.25	*Ret*	63689.6
Ds (m)	1.2192	*Nut*	295.8
lay	1	*ht* (W/m^2 K)	8405.2
ltp (m)	0.03175	*U* (W/m^2 K)	757.3
Ntt	1041.78	*A* (m^2)	405.3
Ntp	260.44	*fs*	0.2437
ebc (m)	0.4433	*ft*	0.02414
Ar (m^2)	0.1081	ΔPs (Pa)	55,584
vs (m/s)	0.92	ΔPt (Pa)	55,573

Table 10
Computational time and problem size.

Case	Area (m^2)	Feasibility	Computational time (s)
1	974.9	Yes	1.6
2	195.2	No	1.6
3	493.6	Yes	123.1
4	405.3	Yes	10.5

The computational time corresponds to the elapsed time using a computer with Intel Core i7 processor with 8 Mb of RAM memory.

The area found using the proposed approach (Case 4) is about 58% smaller than the solution based on the conservative approach (Case 1) and 18% smaller than the best solution obtained in the iterative case (Case 3). The solution found using an optimistic approach for the fouling resistances (Case 2) presents the smallest area, but it is not feasible. The comparison of the computational time indicates that the iterative case is the slowest option and the fixed fouling resistances approach are the fastest. The optimization procedure proposed here is in an intermediate position.

5.6. Optimization considering the total annualized cost

The optimization of the heat exchanger design including the fouling model was also applied using the total annualized cost as objective function. The values used for $\hat{a}_{cost}$ and $\hat{p}_{cost}$ were 123 and 1.31, respectively, and the results obtained are shown in Table 11 associated to a total annualized cost of 15,919 $/year.

As we can see, the results considering in this case were different from case 4, which only considers the minimization of the area. In

Table 8
Best result for the iterative procedure.

Variable	Value	Variable	Value
dte (m)	0.03810	*Deq* (m)	0.0275
dti (m)	0.03480	*Res*	33115.4
L (m)	6.0976	*Nus*	183.6
Nb	13	*hs* (W/m^2 K)	4194.1
Npt	6	*vt* (m/s)	1.864
rp	1.25	*Ret*	93359.6
Ds (m)	1.3716	*Nut*	401.6
lay	2	*ht* (W/m^2 K)	7248.2
ltp (m)	0.047625	*U* (W/m^2 K)	610.9
Ntt	677	*A* (m^2)	493.6
Ntp	112.833	*fs*	0.2442
ebc (m)	0.4355	*ft*	0.0226
Ar (m^2)	0.11948	ΔPs (Pa)	59,734
vs (m/s)	0.837	ΔPt (Pa)	58,047

Table 11
Results for case 5.

Variable	Value	Variable	Value
dte (m)	0.03175	*Deq* (m)	0.02291
dti (m)	0.02845	*Res*	21288.5
L (m)	6.0976	*Nus*	144.03
Nb	11	*hs* (W/m^2 K)	3947.15
Npt	4	*vt* (m/s)	1.05
rp	1.25	*Ret*	42843.8
Ds (m)	1.524	*Nut*	215.4
lay	2	*ht* (W/m^2 K)	4754.6
ltp (m)	0.03969	*U* (W/m^2 K)	409.7
Ntt	1203	*A* (m^2)	731.3
Ntp	300.75	*fs*	0.2654
ebc (m)	0.5081	*ft*	0.02597
Ar (m^2)	0.1549	ΔPs (Pa)	44,145
vs (m/s)	0.646	ΔPt (Pa)	15,702

Case 5, the area is 80% bigger than the area obtained in Case 4 and the tube-side and shell-side pressure drops are 73% and 26% lower, respectively, i.e. the tradeoff between area and pressure drop is considerable different in the two cases.

6. Conclusions

Fouling is an unsolved problem in heat transfer technology. The intensity of the fouling problem depends on the thermofluidynamic conditions associated to the heat exchanger design. However, this aspect of the problem is ignored by the conventional design approach, which is based on the adoption of fixed values of fouling resistances. Therefore, the opportunity to include fouling models at the design phase is the central point of this paper. An important additional aspect of the proposed approach is the utilization of a linear model, which guarantees the identification of the global optimum. This proposal can be applied to the two main representations of the design problem: the minimization of the heat exchanger area or the total annualized cost. Numerical tests for the comparison of the results obtained using our approach and alternative procedures based on fixed fouling resistances or iterative procedures indicates that this proposal can attain better solutions.

Appendix A. Supplementary material

Supplementary data associated with this article can be found, in the online version, at http://dx.doi.org/10.1016/j.applthermaleng.2017.07.066.

References

[1] D.Q. Kern, Process Hear Transfer, McGraw-Hill, New York, 1950.
[2] R.W. Serth, Process Heat Transfer: Principles and Applications, Elsevier, Oxford, 2007.
[3] E. Cao, Heat Transfer in Process Engineering, McGraw-Hill, New York, 2009.
[4] A.C. Caputo, P.M. Pelagagge, P. Salini, Heat exchanger optimized design compared with installed industrial solutions, Appl. Therm. Eng. 87 (2011) 371–380.
[5] T.K. Poddar, G.T. Polley, Heat exchanger design through parameter plotting, Trans. Inst. Chem. Eng. 74 (Part A) (1996) 849–852.
[6] K. Muralikrishna, U.V. Shenoy, Heat exchanger design targets for minimum area and cost, Trans. Inst. Chem. Eng. 78 (Part A) (2000) 161–167.
[7] P.D. Chaudhuri, U.M. Diwekar, J.S. Logsdon, An automated approach for the optimal design of heat exchangers, Ind. Eng. Chem. Res. 36 (1997) 3685–3693.
[8] J.M. Ponce-Ortega, M. Serna-González, A. Jiménez-Gutiérrez, Use of genetic algorithms for the optimal design of shell-and-tube heat exchangers, Appl. Therm. Eng. 29 (2009) 203–209.
[9] V.K. Patel, R.V. Rao, Design optimization of shell-and-tube heat exchanger using particle swarm optimization technique, Appl. Therm. Eng. 30 (2010) 1417–1425.
[10] F.O. Jegede, G.T. Polley, Optimum heat exchanger design, Trans. Inst. Chem. Eng. 70 (Part A) (1992) 133–141.
[11] M. Reppich, J. Kohoutek, Optimal design of shell-and-tube heat exchangers, Compos. Chem. Eng. 18 (Suppl) (1994) S295–S299.
[12] F.T. Mizutani, F.L.P. Pessoa, E.M. Queiroz, S. Hauan, I.E. Grossmann, Mathematical programming model for heat-exchanger network synthesis including detailed heat-exchanger designs. 1. Shell-and-tube heat-exchanger design, Ind. Eng. Chem. Res. 42 (2003) 4009–4018.
[13] J.M. Ponce-Ortega, M. Serna-González, L.I. Salcedo-Estrada, A. Jiménez-Gutiérrez, Minimum-investment design of multiple heat exchangers using a MINLP formulation, Chem. Eng. Res. Des. 82 (2006) 905–910.
[14] M.A.S.S. Ravagnani, J.A. Caballero, A MINLP model for the rigorous design of shell and tube heat exchangers using the Tema standards, Chem. Eng. Res. Des. 85 (2007) 1423–1435.
[15] C.O. Gonçalves, A.L.H. Costa, M.J. Bagajewicz, Shell and tube heat exchanger design using mixed-integer linear programming, AIChE J. (2016), http://dx.doi.org/10.1002/aic.15556.
[16] C.O. Gonçalves, A.L.H. Costa, M.J. Bagajewicz, Alternative MILP formulations for shell and tube heat exchanger optimal design, Ind. Eng. Chem. Res. 56 (2017) 5970–5979.
[17] R.L. Schilling, Fouling and uncertainty margins in tubular heat exchanger design: an alternative, Heat Transfer Eng. 33 (2012) 1094–1104.
[18] D. Butterworth, Design of shell-and-tube heat exchangers when the fouling depends on local temperature and velocity, Appl. Therm. Eng. 22 (2002) 789–801.
[19] D.I. Wilson, G.T. Polley, S.J. Pugh, 2005, Ten years of Ebert, Panchal and the threshold fouling concept, in: Proceedings of International Conference on Heat Exchanger Fouling and Cleaning, 2005, Kloster Irsee, Germany, pp. 25–36.
[20] D.I. Wilson, E.M. Ishiyama, G.T. Polley, 2015, Twenty years of Ebert and Panchal – What next? in: Proceedings of International Conference on Heat Exchanger Fouling and Cleaning, 2005, 2015, Einsfield, Ireland, pp. 1–12.
[21] G.T. Polley, D.I. Wilson, B.L. Yeap, S.J. Pugh, Use of crude oil fouling threshold data in heat exchanger design, Appl. Therm. Eng. 22 (2002) 763–776.
[22] G.T. Polley, A.M. Fuentes, S.J. Pugh, Design of shell-and-tube heat exchangers to achieve a specified operating period in refinery preheat trains, Heat Transfer Eng. 32 (2011) 314–319.
[23] A. Nakao, A. Valdman, A.L.H. Costa, M.J. Bagajewicz, E.M. Queiroz, Incorporating fouling modeling into shell-and-tube heat exchanger design, Ind. Eng. Chem. Res. 56 (2017) 4377–4385.
[24] E.A.D. Saunders, Heat Exchangers: Selection, Design and Construction, John Wiley & Sons, New York, 1988.
[25] F.P. Incropera, D.P. DeWitt, T.L. Bergman, A.S. Lavine, Fundamentals of Heat and Mass Transfer, 6th ed., John Wiley & Sons, 2006.
[26] J. Taborek, Input data and recommended practices, in: E.U. Schlünder (Ed.), Heat Exchanger Design Handbook, Begell House, New York, 1983, pp. 3.3.3-1–3.3.3-5.
[27] J. Taborek, Performance evaluation of a geometry specified exchanger, in: E.U. Schlünder (Ed.), Heat Exchanger Design Handbook, Begell House, New York, 1983, pp. 3.3.9-1–3.3.9-6.
[28] W. Ebert, C.B. Panchal, Analysis of Exxon crude-oil-slip stream coking, Proc Mitigation of Fouling in Industrial Heat Exchangers, San Luis Obispo, USA, 1995, pp. 451–460.
[29] C.B. Panchal, W.C. Kuru, C.F. Liao, W.A. Ebert, J.W. Palen, Threshold conditions for crude oil fouling, in: T.R. Bott, L.F. Melo, C.B. Panchal, E.F.C. Somerscales (Eds.), Understanding Heat Exchanger Fouling and its Mitigation, Begell House, New York, 1999, pp. 273–279.
[30] G.T. Polley, D.I. Wilson, B.L. Yeap, S.J. Pugh., Evaluation of laboratory crude oil threshold fouling data for application to refinery pre-heat trains, Appl. Therm. Eng. 22 (2002) 777–788.
[31] M.R.J. Nasr, M.M. Givi, Modeling of crude oil fouling in preheat exchangers of refinery distillation units, Appl. Therm. Eng. 26 (2006) 1572–1577.
[32] J. Nesta, C.A. Bennett, Reduce fouling in shell-and-tube heat exchangers, Hydrocarbon Process. July (2005) 77–82.
[33] A.C. Caputo, P.M. Pelagagge, P. Salini, Joint economic optimization of heat exchanger design and maintenance policy, Appl. Therm. Eng. 31 (2011) 1381–1392.